ELSEVIER

Journal of Alloys and Compounds 262–263 (1997) 299–304

Journal of ALLOYS AND COMPOUNDS

X-ray powder diffraction study of the stability of solid solutions in $LaO(Cl_{1-x}Br_x)$

Jorma Hölsä[a], Mika Lastusaari[a,*], Jussi Valkonen[b]

[a] *Department of Chemistry, University of Turku, FIN-20014 Turku, Finland*
[b] *University of Jyväskylä, Department of Chemistry, P.O. Box 35, FIN-40351 Jyväskylä, Finland*

Abstract

The formation of solid solutions in the $LaO(Cl_{1-x}Br_x)$ series was studied by X-ray powder diffraction (XPD), Rietveld profile refinement and bond valence calculations. The $LaO(Cl_{1-x}Br_x)$ ($0 \le x \le 1$, step 0.2, and $x = 0.5$) powder samples were prepared by the solid state reaction between La_2O_3 and a mixture of ammonium chloride and bromide. The X-ray powder diffraction patterns were collected at room temperature between 5 and 125° in 2Θ using Cu K_{α_1} radiation ($\lambda = 1.5406$ Å). The XPD data between 20 and 90° were analyzed with the DBWS-9006PC Rietveld profile refinement program. All the $LaO(Cl_{1-x}Br_x)$ phases studied crystallize in the tetragonal PbFCl-type structure with the space group $P4/nmm$ (No. 129). The cell parameters a and c, the z-coordinate of the halide, the La–ligand distances as well as the R-values increased, and the z-coordinate of the lanthanum atom decreased rather smoothly, even if not completely linearly, with increasing bromine content. The global instability index (GII) yielded values below 0.2, indicating complete solid solubility in the system, but showed a local maximum in the middle of the series. © 1997 Elsevier Science S.A.

Keywords: Bond valence; Rare earth oxyhalides; Rietveld analysis; Solid solutions; X-ray powder diffraction

1. Introduction

The luminescent materials based on the rare earths (RE) – either as a dopant or as a host – have now replaced almost all other compounds as commercial phosphors. Among the most efficient host lattices are the RE oxycompounds corresponding to the general formula $(REO)_nX$ where the anion is usually rather simple, i.e. oxygen, halogen or sulphur [1]. The efficiency and stability of the RE oxycompounds as luminescence materials is probably due to the rigid $(REO)_n^{n+}$ complex cation. There exist two $(REO)_n^{n+}$ types of different structure: The most common is the tetragonal structure where the ORE_4 tetrahedra are two-dimensionally linked, and the trigonal-type with three-dimensionally linked tetrahedra [2]. The RE oxyhalide series contains species which correspond to both types [3] and the system can thus be used as model compounds to investigate the reasons for the efficiency and stability of these luminescent materials [4]. As an integral part of the study, the solid solubility and the possible non-stoichiometry as a result of the breakdown of the solid solutions should also be investigated.

In previous parts of our work [5–11], the main emphasis was placed on the study of the cation solid solubility which is essential in modifying the luminescent properties of the particular host and also responsible for the efficiency of the luminescence through

* Corresponding author. Tel.: +358 2 333 6736; fax: +358 2 333 6730; e-mail: miklas@utu.fi

0925-8388/97/$17.00
PII S0925-8388(97)00469-6

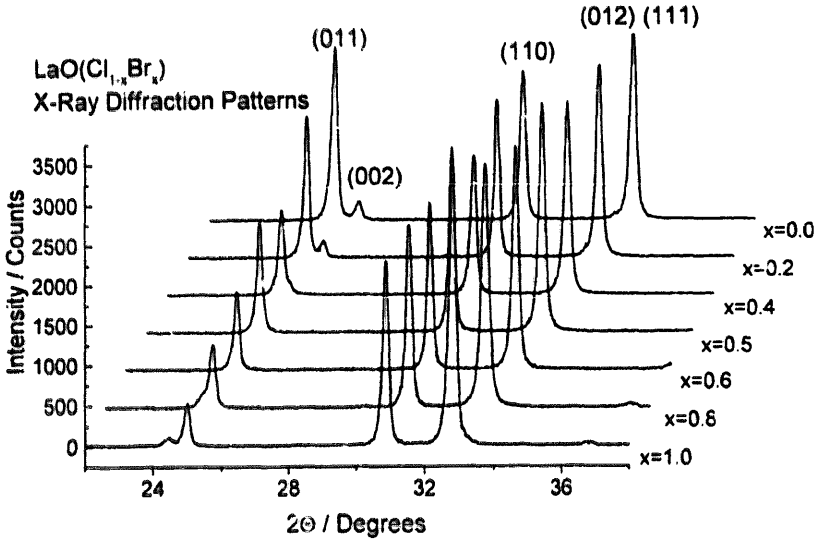

Fig. 1. Room temperature X-ray powder diffraction (XPD) patterns for the $LaO(Cl_{1-x}Br_x)$ phases.

the uniform and random distribution of the dopant. Since it is anticipated that anion substitution will modify the properties of the luminescence material to a greater extent than cation substitution, in the present work anion solid solubility in the $LaO(Cl_{1-x}Br_x)$ series was studied by X-ray powder diffraction (XPD), Rietveld analysis and bond valence calculations.

2. Experimental

2.1. Sample preparation

The $LaO(Cl_{1-x}Br_x)$ phases were prepared by solid state reaction between high-purity (99.99%) La_2O_3 and a mixture of ammonium chloride and bromide at 450°C for 0.5 h followed by recrystallization at 900°C in a static N_2 atmosphere [12]. The NH_4X/La_2O_3 ratio was 2.10. The initial NH_4Cl/NH_4Br ratios were chosen in such a manner that the bromine content varied between 0.0 and 1.0 (step 0.2) except for the 1:1 composition. The $LaO(Cl_{1-x}Br_x)$ phases were doped with a small amount (1 mol-%) of Eu^{3+} for the eventual luminescence measurements. This slight doping should not cause any problems in the formation of the $(Cl_{1-x}Br_x)$ solid solutions and the subsequent XPD analysis.

2.2. X-ray powder diffraction

The X-ray powder diffraction patterns of the $LaO(Cl_{1-x}Br_x)$ samples were recorded with a ENRAF-NONIUS PDS120 X-ray powder diffractometer (Cu K_{α_1} radiation, $\lambda = 1.5406$ Å) equipped with a INEL CPS120 position sensitive detector (Fig. 1). The measurements were carried out at room temperature between 5 and 125° in 2θ using a flat rotating sample holder. A mixture of silicon and mica (flogopite) powders was used as an external standard up to ca. 95°. The angular resolution of the apparatus was better than 0.018°.

2.3. Rietveld profile refinement

The XPD data were analyzed with the Rietveld profile refinement method [13] using the DBWS-9006PC program [14]. The Rietveld method employs total pattern fitting between the observed and calculated intensity for every data point in the diffraction pattern. The Rietveld analyses were performed with the data between 20 and 90° in 2θ (Fig. 2). The unit cell, atom position, pseudo-Voigt profile form, profile asymmetry, background (a fifth-order polynomial function) and isotropic temperature parameters were all refined, but not always simultaneously. The pseudo-Voigt profile function was corrected for

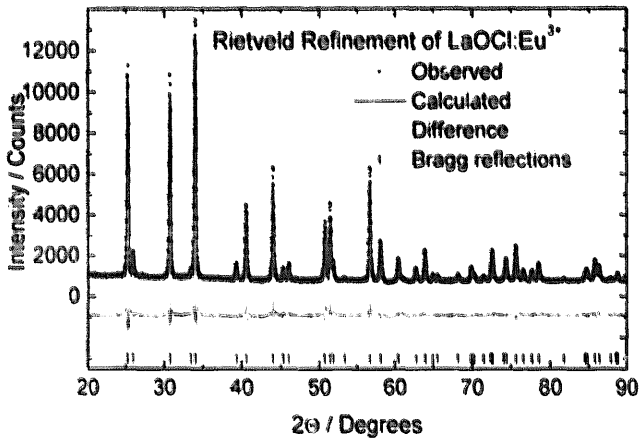

Fig. 2. Results of the Rietveld profile refinement analysis of the X-ray powder diffraction pattern of the LaOCl phase.

Table 1
Rietveld refinement results for the $LaO(Cl_{1-x}Br_x):Eu^{3+}$ series

Parameter	LaOCl	$LaOCl_{0.8}Br_{0.2}$	$LaOCl_{0.6}Br_{0.4}$	$LaOCl_{0.5}Br_{0.5}$	$LaOCl_{0.4}Br_{0.6}$	$LaOCl_{0.2}Br_{0.8}$	LaOBr
a (Å)	4.11621(1)	4.12439(1)	4.13237(2)	4.13583(2)	4.13801(1)	4.14271(2)	4.14792(2)
c (Å)	6.87460(3)	6.96331(3)	7.06931(3)	7.12429(4)	7.18000(4)	7.28947(4)	7.39280(4)
V (Å^3)	116.61	118.14	120.59	122.03	123.06	124.95	127.27
z(La)	0.1748(2)	0.1723(2)	0.1699(2)	0.1679(3)	0.1664(3)	0.1647(3)	0.1615(3)
z(X)	0.6313(8)	0.6326(7)	0.6327(6)	0.6349(8)	0.6313(8)	0.6330(6)	0.6367(5)
B(La) (Å^2)	0.3555(493)	0.3150(548)	0.4622(513)	0.4407(560)	0.5416(565)	0.2737(640)	0.3821(660)
B(X) (Å^2)	1.0130(1444)	0.8922(1228)	0.5623(820)	0.5813(1133)	0.3650(1178)	0.7025(1007)	0.7442(980)
B(O) (Å^2)	1.0272(3446)	1.0603(3761)	0.9598(3952)	0.0056(4015)	0.1044(4328)	0.5082(4699)	0.9868(5401)
R_{wp} (%)	7.20	7.42	7.68	8.20	8.60	9.07	9.71
R_B (%)	6.91	6.89	7.65	7.66	7.52	8.25	8.04
La–O (Å)	2.383(1)	2.386(1)	2.390(1)	2.389(1)	2.389(1)	2.394(1)	2.393(1)
La–X (×4) (Å)	3.201(2)	3.217(2)	3.238(2)	3.244(3)	3.267(3)	3.280(2)	3.293(2)
La–X (×1) (Å)	3.138(6)	3.205(5)	3.272(4)	3.327(6)	3.338(6)	3.414(5)	3.508(4)
GII	0.185	0.173	0.156	0.162	0.160	0.142	0.153

asymmetry for all reflections with 2θ less than 90°. The detailed parameter refinement scheme has been described in detail elsewhere [15].

The least-squares calculations were carried out until a constant R_{wp} value was obtained in the refinement between the entire observed and calculated powder diffraction pattern. The R_{wp} values, used as a figure of merit of the refinement, varied between 7.2 and 9.7% (Table 1) and are satisfactory. The use of R_{wp} values is, however, contested and a better description of the quality of the fit is probably given by the Bragg R value R_B [16], although this is affected by the overlap of reflections. For the $LaO(Cl_{1-x}Br_x)$ system the degree of overlap, fortunately, is insignificant. The R_B values increased slightly with increasing bromine content, which is rather difficult to correlate to any obvious feature in the XPD patterns.

2.4. Bond valence model calculations

The bond valence model provides a useful and quantitative description of inorganic bonding in ionic solids [17,18]. In this model, the sum of the bond valences calculated from the experimental structural data for each ion in the structure is compared with its nominal valence. The difference between the bond valence and the nominal valence describes the strains present in the compound. In compounds with bonds of intermediate strength (e.g., the oxides and halides of di- and trivalent cations), the relaxation of the strains can result in non-stoichiometry, stabilization of unusual oxidation states, distortions in bonding or lowering of the crystal symmetry [19]. With the aid of the bond valence concept, detailed insight into the inherent instability of compounds, or of the instability of a crystal structure vis-à-vis another polymorph, can be obtained for an individual compound [20] or for a series of compounds [21].

The bond valences, s_{ij}, for each cation–anion pair can be obtained from a comparison between the experimental interatomic bond distances R_{ij} and their characteristic distance R_0 [22]:

$$s_{ij} = \exp\left[(R_0 - R_{ij})/B\right], \quad (1)$$

where B is a universal constant equal to 0.37 [22]. The R_0 values for the most frequent cation–anion pairs for oxides and halides can be found in the literature [18,23].

The global instability index (GII) (Eq. (2)) derived from the bond valence model can be used to estimate the stability of the structure studied [20]. This quantity is defined by a further comparison between the calculated bond valences s_{ij} and the formal valence V_i for all the species N in the asymmetric unit of the unit cell [20]:

$$\mathrm{GII} = \left\{ \sum_{i=1}^{N} \left[(\Sigma_j s_{ij} - V_i)^2 / N \right] \right\}^{1/2}. \quad (2)$$

The global instability index also describes the strains in the structure and places a limit on the maximum allowable distortion. According to an empirical formulation, with GII values exceeding 0.2 the structure becomes unstable and faces a possible collapse or a phase transformation [24].

3. Results and discussion

3.1. Structure refinement

The XPD patterns of the $LaO(Cl_{1-x}Br_x)$ series show no significant changes between the different members of the series (Fig. 1), only a smooth variation of the reflection positions and intensities can be

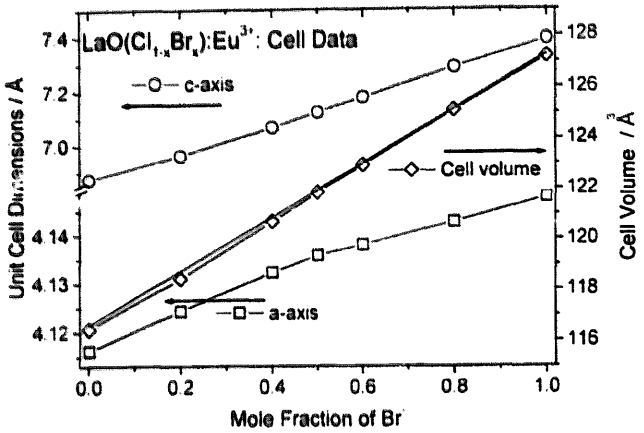

Fig. 3. Evolution of the unit cell parameters in the $LaO(Cl_{1-x}Br_x)$ series. The straight line in the cell volume was interpolated between pure LaOCl and LaOBr. The errors in the parameters are smaller than the symbol heights.

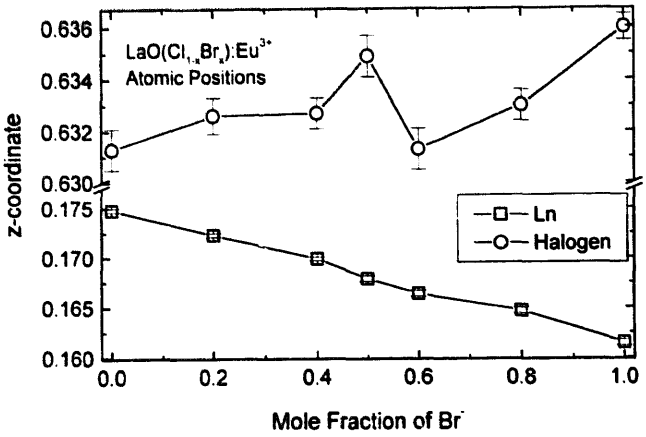

Fig. 4. Evolution of the atomic coordinates in the $LaO(Cl_{1-x}Br_x)$ series.

observed. No splitting of the reflections or the appearance of new reflections indicating the formation of other than the conventional solid solutions could be observed. The absence of significantly different XPD patterns for any of the intermediate phases was to be expected because of the similar structure of LaOCl and LaOBr and the small difference in the ionic radii of the two host anions, i.e. 1.81 vs. 1.96 Å [25] for Cl^- and Br^-, respectively.

All the members of the $LaO(Cl_{1-x}Br_x)$ series crystallize in the tetragonal space group $P4/nmm$ (No. 129 [26]; $Z = 2$) with a structure similar to the natural mineral matlockite, PbFCl [27,28]. The lanthanum atom is coordinated to four oxygens and five chlorines (one on the four-fold axis) in a monocapped tetragonal antiprism arrangement yielding C_{4v} as the point symmetry of the lanthanum site.

The structure refinements were carried out successfully (Table 1). As pointed out above, the R values are satisfactory for complicated systems such as the presumed $LaO(Cl_{1-x}Br_x)$ solid solutions. Better results could perhaps have been obtained by increasing the measuring time as the statistics of the experimental data would have been improved. The lowest R values were obtained for the LaOCl phase, probably due to the best crystallinity in the sample series. On the other hand, the intensity of the reflections increased with increasing bromide content. The esd's of the calculated parameters are very low with the exception of the values for the isotropic thermal parameters. In powder diffraction work all discrepancies tend to accumulate on these parameters, but despite this the actual values of the parameters are plausible, which is not always the case.

A more quantitative description of the solid solubility in the $LaO(Cl_{1-x}Br_x)$ series requires a careful analysis of the results of the Rietveld refinements. The smooth and practically linear evolution of the unit cell parameters a and c (Fig. 3) indicates complete solid solubility. However, a slight curvature could be observed in the middle of the series, but the cell volume remained constant in this region. The cell volume deviated from linearity at low x_{Cl} and x_{Br} values in the beginning and at the end of the series. The deviations were very small, but clustering of anions may still occur due to the positive deviation of the value of the a parameter from linearity as a function of the substitution rate [29]. Complete breakdown of the solid solubility is, however, in disagreement with Vegard's law since the difference in the ionic radii of the Cl^- and Br^- ions is too small.

Another indication of anomalies in anion substitution in the $LaO(Cl_{1-x}Br_x)$ series comes from the atom position parameters for different atoms. Both the La and chlorine atoms occupy a special two-fold position $(0,\frac{1}{2},z)$, whereas the oxygens reside in a rather similar position (0,0,0) [26]. The total number of refined parameters, i.e. the z-coordinates of the lanthanum and halogen, is thus very low, ensuring reliable results of the refinements. The z_{La} value decreases smoothly with increasing bromine content, indicating the stability of the rigid $(LaO)_n^{n+}$ complex cation (Fig. 4). The z_X parameter shows irregular behavior in the middle of the series, which also indicates anomalies in anion substitution.

Similar conclusions to those given above can be drawn from the La–ligand distances (Fig. 5), which also reveal the eventual change in the coordination of the lanthanum from a strict nine coordination for LaOCl to eight coordination for LaOBr. The dilatation of the whole structure (amounting to 9% as judged from the cell volume) is shown by the increase in the La–X bond length, which is also somewhat irregular in the middle of the series.

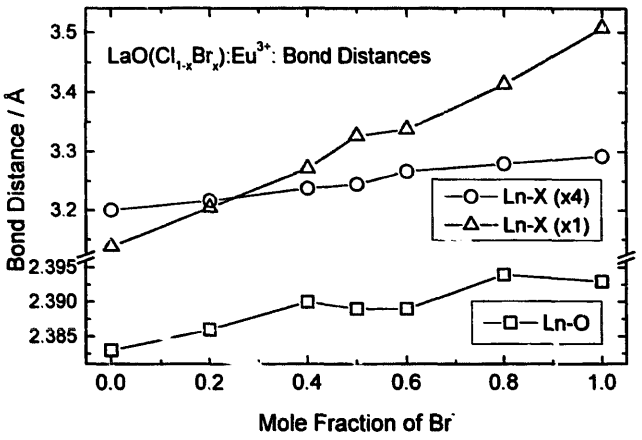

Fig. 5. Evolution of the interatomic RE–ligand distances in the $LaO(Cl_{1-x}Br_x)$ series. The errors in the distances are smaller than the symbol heights.

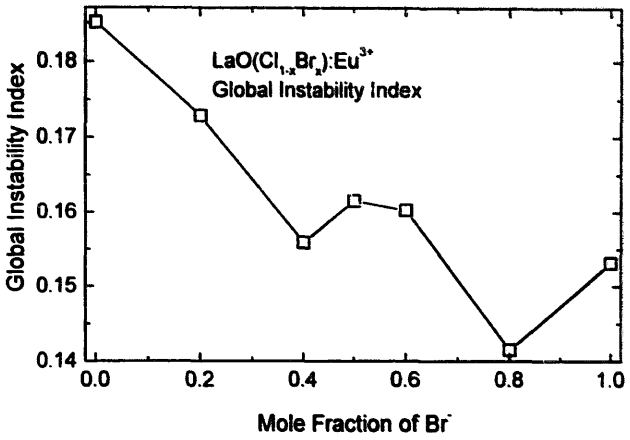

Fig. 6. Evolution of the global instability index (GII) in the $LaO(Cl_{1-x}Br_x)$ series.

3.2. Bond valence calculations

The bond valence concept [17,18] has only infrequently been employed to study the stability of individual crystal structures or the stability of a certain structure in a series of isomorphic compounds. Comparison of the experimental cation–anion bond distances with their characteristic distance and a further comparison of the sum of the calculated bond valences with the nominal valence of the species provides a rather simple formulation to carry out such stability studies. Frequently, the sum of the bond valences (the global instability index, GII) differs significantly from the valence.

No GII value in the $LaO(Cl_{1-x}Br_x)$ series exceeds 0.2, which indicates the stability of all phases, and complete solid solubility should occur in the whole system. The general trend in the GII values is a decrease with increasing bromine content (Fig. 6). There is, however, a local maximum in the middle of the series which reflects well the anomalies found in the structural parameters discussed above.

The GII value is the highest for the pure LaOCl and the lowest for the pure LaOBr phase. This observation can readily be associated with the experimental observation of the stability of the oxychloride and oxybromide phases in general. The tetragonal REOCl structure is stable only up to ErOCl – which is dimorphic [30]. Beyond ErOCl the hexagonal SmSI-type structure can be found for the three heaviest RE oxychlorides [31]. In contrast to the oxychloride series, the oxybromide series is stable throughout the whole RE series [32]. The oxybromide structure is thus more stable than the oxychloride structure. The present bond valence calculations seem to verify this experimental observation and to confirm the utility of the model to predict limits of stabilities of structures in a series of isomorphous compounds.

4. Conclusions

Rietveld analysis of the X-ray powder diffraction patterns of the $LaO(Cl_{1-x}Br_x)$ system revealed complete solid solubility throughout the whole concentration range. The detailed structural information from the Rietveld analyses, i.e. the evolution of the unit cell dimensions, atom position parameters and La–ligand distances, all indicate that local clustering or disorder could occur in the middle – or even at much lower substitution concentrations – of the series. The bond valence model calculations indicate that all intermediate phases between the limiting compositions – LaOCl and LaOBr – are perfectly stable, but there is also a maximum in the instability in the middle of the series. An explanation for the relative instability of the pure oxychloride phase with respect to the corresponding oxybromide phase was also obtained from the bond valence model. This is in agreement with the available experimental data showing an isomorphous REOBr structure throughout the whole RE range while the tetragonal REOCl form does not exist for the three heaviest REs.

The nature of the local disorder in the $LaO(Cl_{1-x}Br_x)$ system cannot be deduced easily from X-ray (powder) diffraction studies since, due to the inherent limitation of the method, only average structural information can be obtained. The careful and quantitative interpretation of the luminescence properties of the Eu^{3+} ion embedded in the $LaO(Cl_{1-x}Br_x)$ system will be of more use in the study of the local structural effects in these solid solutions. This study will be carried out in the near future.

References

[1] P. Porcher, P. Caro, J. Less-Common Met. 93 (1983) 151.
[2] P.E. Caro, J. Less-Common Met. 16 (1968) 367.
[3] W.P. Willmarth, J.R. Peterson, Characterization of selected solid-state actinide (and related) compounds via Raman and absorption spectrophotometry, in: A.J. Freeman, C. Keller (Eds.), Handbook of Physics and Chemistry of Actinides, Elsevier, Amsterdam, 1991, p. 1.
[4] E. Säilynoja, PhD Thesis, University of Turku, Turku, Finland, 1996.
[5] H.-J. Limburg, J. Hölsä, P. Porcher, G. Herzog, D. Starick, H. Wulff, Phys. Status Solidi (a) 130 (1992) K155.
[6] H.-J. Limburg, J. Hölsä, P. Porcher, G. Herzog, D. Starick, H. Wulff, J. Solid-State Chem. 98 (1992) 404.
[7] H.-J. Limburg, J. Hölsä, P. Porcher, G. Herzog, D. Starick, H. Wulff, Philos. Mag. B 67 (1993) 541.
[8] J. Hölsä, E. Kestilä, K. Koski, H. Rahiala, J. Alloys Compounds 91 (1995) 193.
[9] J. Hölsä, E. Säilynoja, K. Koski, H. Rahiala, J. Valkonen, Powder Diffr. 11 (1996) 129.
[10] J. Hölsä, K. Koski, R.-J. Lamminmäki, H. Rahiala, E. Säilynoja, Acta Phys. Pol. A 91 (1997) 563.
[11] J. Hölsä, K. Koski, R.-J. Lamminmäki, E. Säilynoja, P. Dereń, W. Stręk, J. Alloys Compounds 250 (1997) 370.
[12] J. Hölsä, L. Niinistö, Thermochim. Acta 37 (1980) 155.
[13] R.A. Young (Ed.), The Rietveld Method, Oxford University Press, Oxford, 1993.
[14] A. Sakthivel, R.A. Young, Program DBWS-9006PC for Rietveld Analysis of X-ray and Neutron Powder Diffraction Patterns, Georgia Institute of Technology, Atlanta, GA, 1991.
[15] J. Hölsä, E. Kestilä, R. Saez-Puche, P. Dereń, W. Stręk, P. Porcher, J. Phys.: Condensed Matter 8 (1996) 1575.
[16] K. Jansen, W. Schäfer, G. Will, J. Appl. Crystallogr. 27 (1994) 492.
[17] I.D. Brown, D. Altermatt, Acta Crystallogr., Sect. B 41 (1985) 240.
[18] I.D. Brown, D. Altermatt, Acta Crystallogr., Sect. B 41 (1985) 244.
[19] I.D. Brown, Acta Crystallogr., Sect. B 48 (1992) 553.
[20] I.D. Brown, Z. Krist. 199 (1992) 255.
[21] A. Salinas-Sanchez, J.L. Garcia-Muñoz, J. Rodrigues-Carvajal, R. Saez-Puche, J.L. Martinez, J. Solid-State Chem. 100 (1992) 201.
[22] I.D. Brown, Phys. Chem. Miner. 15 (1987) 30.
[23] N.E. Brese, M. O'Keeffe, Acta Crystallogr., Sect. B 47 (1991) 192.
[24] T. Armbruster, F. Röthlisberger, F. Seifert, Am. Mineral. 75 (1990) 847.
[25] R.D. Shannon, Acta Crystallogr., Sect. A 32 (1976) 751.
[26] N.F.M. Henry, K. Lonsdale (Eds.), Int. Tables Crystallography, Vol. 1, Kynoch Press, Birmingham, 1969.
[27] L.G. Sillén, A.L. Nylander, Svensk Kem. Tidskr. 53 (1941) 367.
[28] L.H. Brixner, E.P. Moore, Acta Crystallogr., Sect. C 39 (1983) 1316.
[29] M. Castellanos, A.R. West, J. Chem. Soc., Faraday Trans. 76 (1980) 2159.
[30] D.H. Templeton, C.H. Dauben, J. Am. Chem. Soc. 75 (1953) 6069.
[31] H.P. Beck, Z. Naturforsch. 31b (1976) 1562.
[32] I. Mayer, S. Zolotov, F. Kassierer, Inorg. Chem. 4 (1965) 1637.